DØ note 5333
Fermilab-TM-2444-PPD

Design and Analysis for the Carbon Fiber Composite Support Structure for Layer 0 of the DØ Silicon Micro Tracker

C. H. Daly, Mark E. Tuttle and William Kuykendall, Department of Mechanical Engineering, University of Washington, Seattle

The support structures for the new Layer 0 (Figures 1, 2, 3) of the Run 2b silicon tracker in D0 were designed and fabricated at the University of Washington. These structures were required to have minimum mass, yet be very rigid so as to meet the high precision requirements placed on the position of the silicon detector chips. They also have to provide for cooling to remove the heat generated by the sensors and signal processing electronics and to keep the sensors at the desired operating temperature (below -5 C).

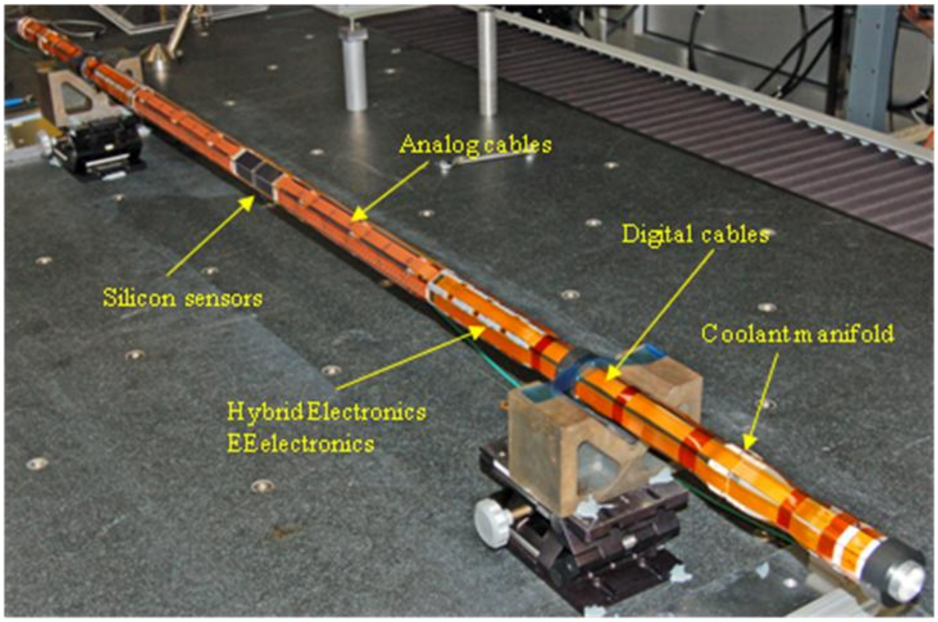

Fig. 1 Completed Layer0 detector

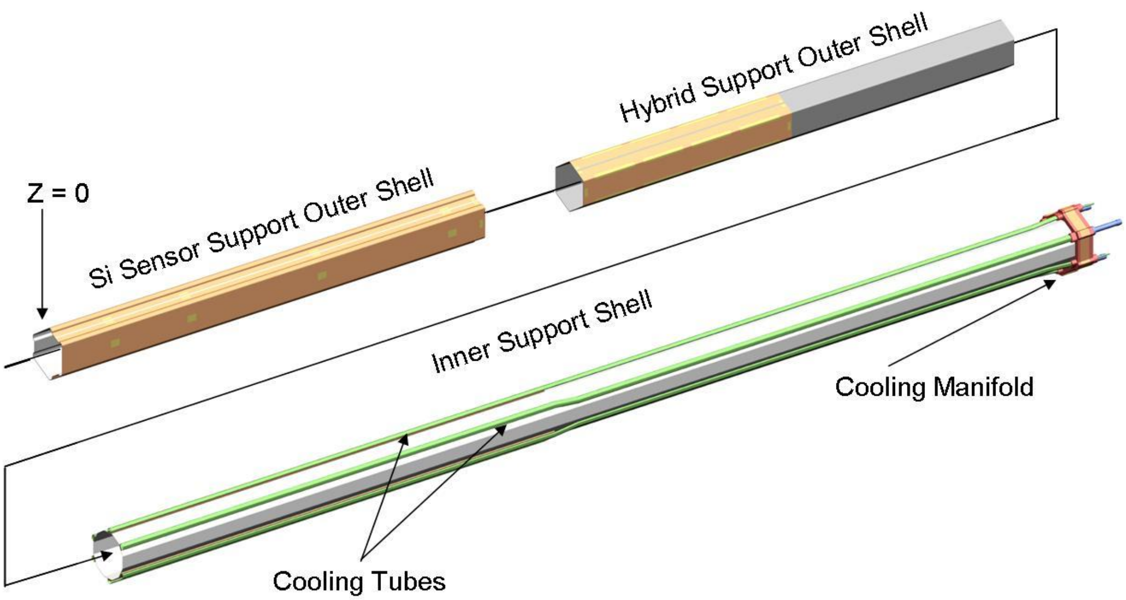

Fig. 2. Exploded view of LØ shell assembly. Half-structure shown.

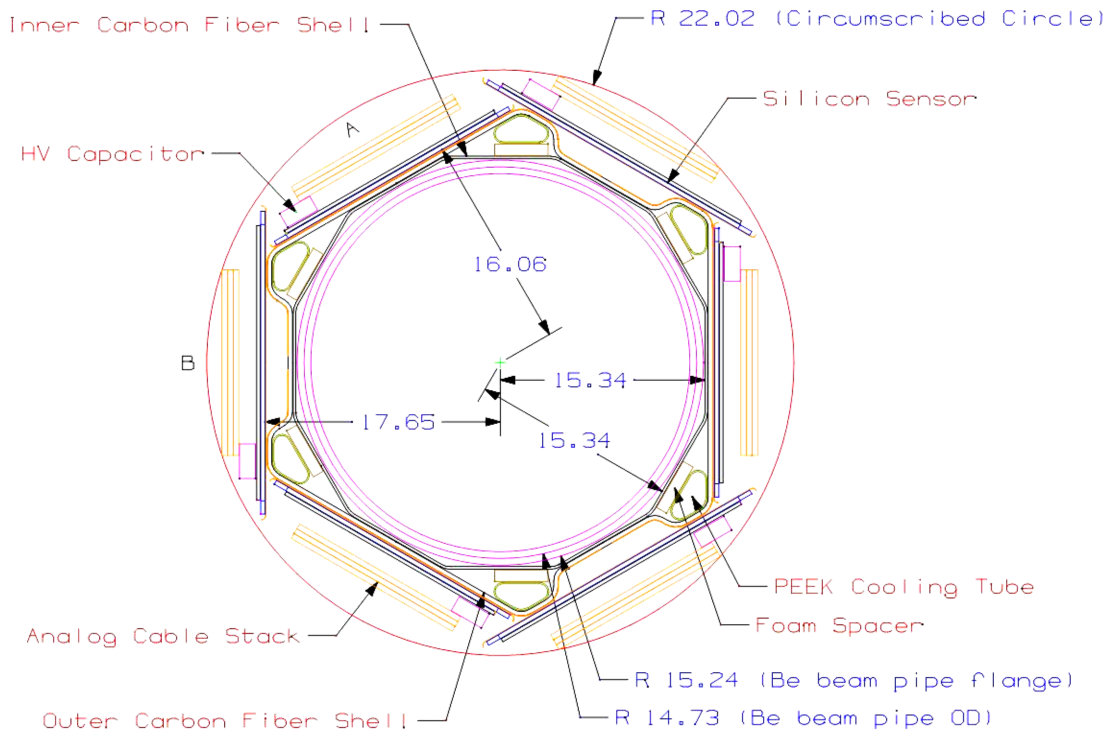

Fig. 3. Cross-section of sensor region.

All of these requirements were best met by carbon fiber/epoxy composite technology. State of the art carbon fiber materials have extremely high Young's moduli and high thermal conductivity.

Appropriate fiber lay-ups and fabrication methods have been developed and used successfully to produce both various prototype structures and the structures used in the production Layer 0. The geometry of these structures was determined mainly by the geometry of the sensors themselves[3]. The structures incorporated a complete cooling system consisting of extruded PEEK coolant tubes and distribution manifolds made from carbon fiber composites.

In order to determine the mechanical and thermal performance of the structures, detailed FEA analyses of L0 have been carried out and are described below.

FEA – methods

All of the FEA work was done using Ansys® software, a very powerful package that can handle both the stress and deflection analysis and the thermal (heat flow) analysis needed.

The first stage of FEA was to create the geometry of the model in such a way as to facilitate the application of the desired mechanical and thermal properties to each part of the structure, the sensors, hybrid circuits and cooling system. The simplest way to do this was to take the geometry from the CAD (Unigraphics NX) 3-d model and transfer it into Ansys using an intermediate Parasolid file. This was quick and simple but did require that any changes in the geometry be done in the CAD world and then re-meshed in Ansys. In those cases where it was necessary to vary the geometry parameters several times, the FEA geometry was build directly in Ansys using its parametric input language. While this took longer, changes could be made very simply as many times as needed. The end result was the same with either method.

Mechanical and Thermal Properties

Many different material properties were needed in these models and are given in Tables 1 and 2.

Table 1: Mechanical properties used in FEA Models

Material	Elastic Moduli									Density
	E_x - GPa	E_y - GPa	E_z - GPa	G_{xy} - GPa	G_{yz} - GPa	G_{xz} - GPa	ν_{xy}	ν_{yz}	ν_{xz}	kg/m^3
Carbon fiber - outer shells	265	36	6	36.8	4.1	4.1	3	0.1266	-0.0089	1554
Carbon fiber - inner shell	276	141	6.7	20	4.1	4.1	0.0084	0.0078	0.0047	1554
PEEK - coolant tubes	4.5						0.4			1330
Silicon	110						0.3			2330
Epoxy	2.6						0.3			1200
Epoxy/Kapton layers	2.7						0.3			1280

Table 2: Thermal Properties used in FEA models

Material	Thermal Conductivities			Density	Spec. Heat
	k_x - W/mK	k_y - W/mK	k_z - W/mK	kg/m^3	J/kgK
Carbon fiber - castellated shell	408	43	0.73	1554	
Carbon fiber - inner shell	343	110	0.73	1554	
PEEK - coolant tubes	0.25			1330	
Silicon	125			2330	
Epoxy	0.2			1200	
Conductive epoxy	9			1200	
Epoxy/Kapton layers	0.1733	0.1733	0.1636	1310	
Coolant	0.3707			1089	3307
Borosilicate glass	1.4			2223	
BeO	280			2900	
SiN spacers	30			2495	

Note that two sets of orthotropic carbon fiber properties were needed because of the different fiber lay-ups used in the inner and outer shells. All of these properties were predicted from the pre-preg properties, given by the manufacturer, using standard composite layup theory. All components of the structure were produced using pre-preg materials and hand lay-up. Pre-preg materials were custom-ordered from YLA Inc. A pre-preg based on K13C2U fibers and a modified epoxy resin matrix was used to produce the castellated and hexagonal tubes and is designated as K13C2U /RS-24 in the following discussion.

Stacking Sequences and Material Properties

Different stacking sequences were used in the outer castellated and hexagonal tubes and the dodecagonal inner tube. Fiber angles were referenced to the longitudinal axis, e.g., fibers within a $0°$ ply were parallel to the long axis of the tubes. Symmetric stacking sequences were used throughout the structure to eliminate thermal warping. As is evident from Fig. 3, fibers in the outer castellated tubes were required to conform to several corners of small radius. Ply fiber angles were limited to about $\pm 20°$ to avoid fiber fracture at and near these corners. A stacking sequence of +20/-20/0/-20/20° was selected for use in the outer castellated tube. The outer tube therefore possessed high axial and shear stiffness, but very low circumferential stiffness. Since the inner hexagonal tube was produced without sharp corners, fiber angles of any value could be used in this tube. A stacking sequence of 0/90/0° was selected, which provided high axial and circumferential stiffness. The predicted properties were verified by mechanical testing of sample specimens as described elsewhere.

Advantage was taken of the symmetry of the structure. For the mechanical model, only one half of the actual structure was required. For the thermal model in the hybrid region of the structure, only one sixth of one end of the structure was needed.

Mechanical FEA

The principal goal here was to confirm that the deflection of the structure under gravitational and thermal loads was within the design requirements. Because of the low weights of the structures, stresses were very low and not a significant issue. Likewise, buckling analysis showed that there was no problem in this regard even with these very thin wall structures.

As described below, finite element analyses were used throughout the design process. These analyses were based on effective laminate properties, which were themselves predicted using unidirectional ply properties and classical lamination theory (CLT). A limited experimental study was performed to measure ply properties and also to verify that CLT could be used to predict multi-angle laminate properties to within engineering accuracies. Since a very limited supply of pre-preg was available, only a single measurement was made of each property. Single ply properties were first measured for the K13C2U/RS-24 material system. The fiber dominated Young's modulus and the major Poisson ratio, E_{11} and ν_{12} respectively, were inferred from strains measured using biaxial strain gauges mounted back-to-back on $[0]_n$ specimens. The matrix dominated Young's modulus E_{22} was inferred from strains measured using uniaxial strain gauges mounted back-to-back on $[90]_n$ specimens. The shear modulus G_{12} was inferred from strains measured using biaxial strain gauges mounted back-to-back on $[\pm 45]_{ns}$ specimens. These tests were performed in accordance with ASTM Test Standards D3039 and D3518.[1,2]

Table 3: Ply properties measured for K13C2U/RS-24 pre-preg

Material	E_{11} (GPa)	ν_{12}	E_{22} (GPa)	G_{12} (GPa)
K13C2U/RS-24	410	0.39	5.6	4.1

Having measured ply properties, effective in-plane properties could be predicted for any multi-angle laminate using CLT.[4] The tensile modulus E_{xx}, and Poisson's Ratio ν_{xy} exhibited by a six-ply K13C2U/RS-24 laminate with $[0/\pm 20]_s$ stacking sequence were measured and compared to CLT predictions. These measurements and a comparison to theory are summarized in Table 4. Since only a single measurement of each property listed in Tables 3 and 4 was obtained, these measurements are not valid in a statistical sense. Nevertheless, the trends in effective laminate properties predicted by CLT were verified by measurement. For example, note that the very large value of ν_{xy} predicted for a $[0/\pm 20]_s$ laminate compares well with the measured value.

Table 4: Comparison of measured and predicted properties for a $[0/\pm 20]_s$ K13C2U/RS-24 laminate

Property	Measured	Predicted	Difference (%)
E_{xx} (GPa)	301	265	12
ν_{xy}	3.1	3.0	3.2

The carbon fiber parts of the structure were modeled using the orthotropic mechanical properties given above. These include the outer, 5-layer castellated shells for the sensor regions, the hexagonal outer shells for the hybrid region and the inner, full length 3-layer shell. The orthotropic properties were properly incorporated into the models so that the property directions correctly followed the geometry of the model. The multiple layers of Kapton and epoxy between the carbon composite surface and the underside of the sensors were modeled as a single layer with the elastic moduli and thermal conductivities calculated using the rule of mixtures. The resulting equivalent properties were orthotropic as the through thickness properties were different from the in-plane properties. All other materials were assumed to be isotropic.

The mechanical FEA model of the L0 structure is shown in Figure 4. More detail is shown in Figure 5.

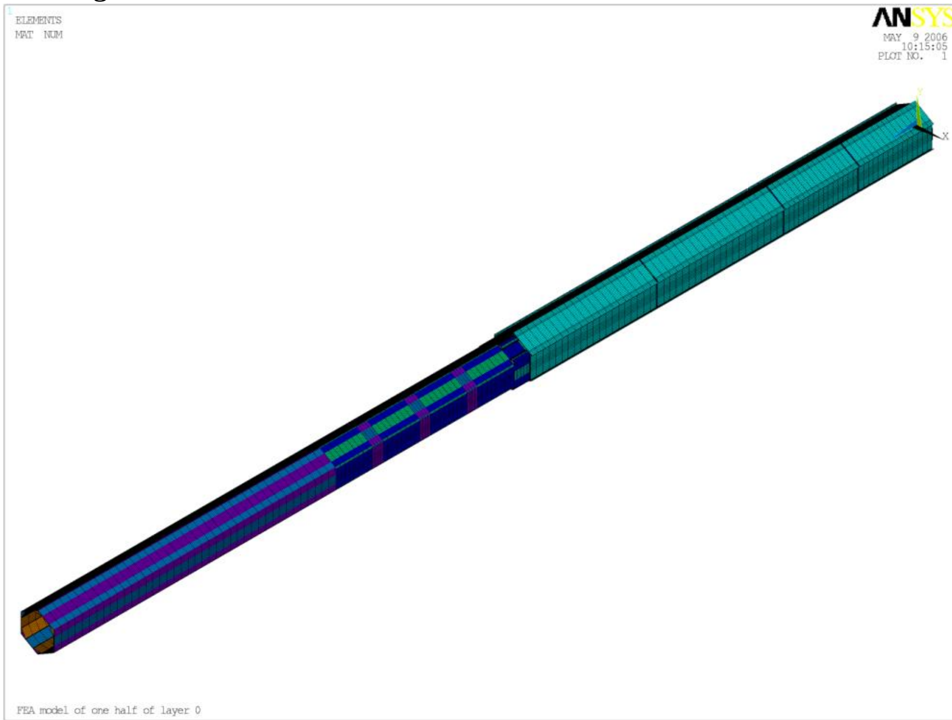

Figure 4: Ansys® FEA model of one Half of Layer0

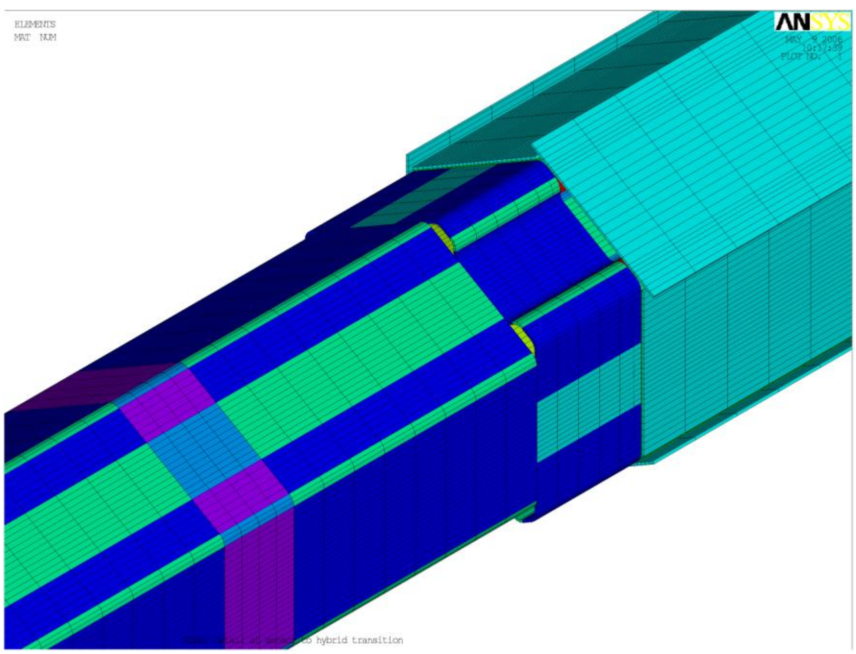

Figure 5: Detail of FEA Model at the Sensor- Hybrid Boundary.

The weights were accounted for by using the appropriate density for each component. For the coolant fluid, the weight was added in by increasing the density of the cooling tubes to give the correct overall weight. The weights of the manifolds and the coolant therein were ignored as the manifolds were at the structure's support points and did not need to be modeled in detail. The cable weight was entered as a distributed load matching the actual cable distribution. The sensors were modeled using the properties of silicon. All epoxy layers were directly modeled except that the epoxy/kapton layers were modeled as one material with calculated equivalent moduli and density. The hybrid substrates were similarly modeled to account for the layers of boro-silicate glass and BeO.

One important use of the FEA analysis was to optimize the fiber lay-ups used in each shell. While deflection was the main consideration, it was also necessary to consider the effects of dimensional changes during the lay-up and cure of the shells to be sure that they could be removed from the tooling. Another consideration was to understand the deflections that would occur under the significant loads used during installation of the sensors on the structure. This analysis led to the design of the internal support tool used in that process[3].

Thermal FEA

Thermal FEA modeling of the silicon detector structures was essential in order to design a cooling system that would keep the silicon sensors and their hybrid circuits within the desired temperature ranges.

There were two distinct thermal loads in the L0 detector:

1. L0 silicon sensor chips. These initially generate little heat that, with time, increases as the chips degrade.
2. L0 hybrid circuits. The hybrid circuits generate significant heat. They are physically separate from the silicon and have much less stringent temperature limits.

The thermal analysis for L0 was done only for the hybrids. The fluid flow comes in at one end of L0, flows through one end section with one half of the hybrids, picking up heat in the process. It then flows through the middle section containing the silicon sensors. It was not expected that these radiation hard chips will degrade over the life of L0 to the point where they will generate significant heat. The silicon sensors thus run at essentially the same temperature as that of the fluid as it enters the sensor region. The fluid then continues through the other end of L0, picking up more heat from that set of hybrids. As the two ends are identical, only one end was modeled.

Each hybrid circuit is almost symmetric about its centerline. One sixth of the circumference of the full length of one hybrid region was modeled as shown in Figures 6 and 7.

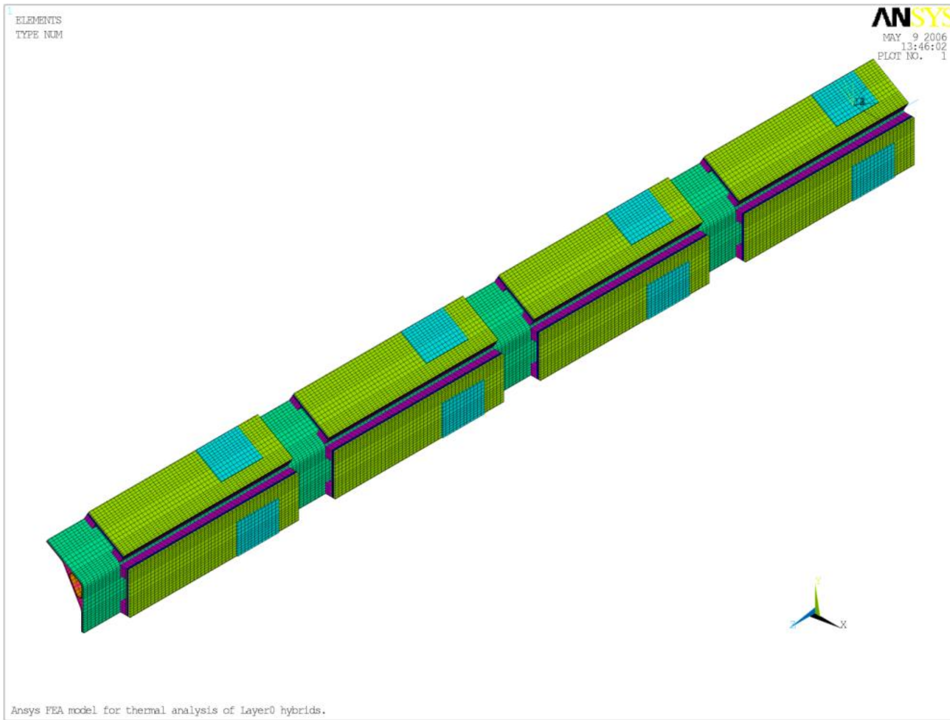

Figure 6: Ansys® FEA Thermal Model of Layer 0 Hybrid Region.

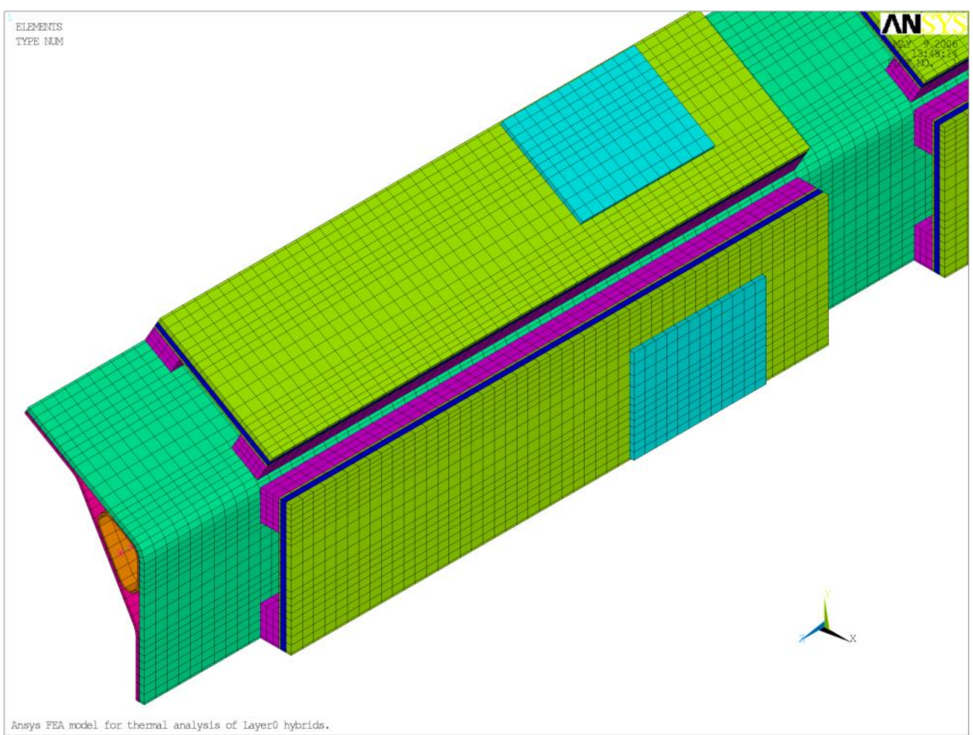

Figure 7: Detail of Model of One Hybrid.

The FEA geometry for the hybrid region model was created in the Unigraphics NX CAD system and transferred to Ansys via a Parasolid file. The model was then meshed and appropriate thermal loads and boundary conditions were applied.

The heat generated by each hybrid chip was modeled by a 0.18 W load applied over the area on the substrate under the chip. The coolant flow enters the cooling tube at -15 °C. Heat convection into this fluid was modeled using surface effect elements coupled to the line elements that represented the flowing coolant. The fluid was taken to be a 40% by volume solution of ethylene glycol in water and the flow velocity in the cooling tubes was 0.1 m/s.

Results

L0 Mechanical

The gravitational deflection of the L0 structure is shown in Figure 8. The maximum sagitta of the sensor region was 158 µm[a]. The deflection in the region of the sensors is shown in Figure 9. The total sag in this region was 38 µm. As this is the critical region, the deviation in sensor position in the installed position in Dzero can be kept to a minimum by offsetting the whole structure upwards by 139 µm. This will result in the actual sensor positions being only ±19 µm from the ideal position.

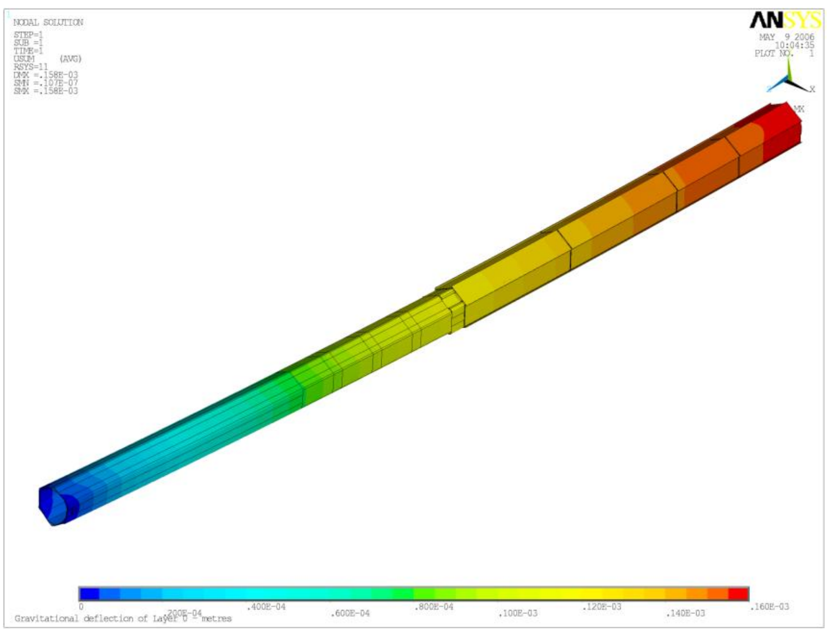

Figure 8: Gravitational Deflection of Layer 0. The Maximum Sagitta is 158 µm at the Mid Point.

---

[a] *In Ansys a pure SI units system is used. All lengths and deflections are in meters and all stresses and pressures in Pascals. In a typical plot below, SMN and SMX are the minimum and maximum values of the plotted variable. UX is displacement in the X-direction in meters and the coordinate system is shown on the plot. SEQV is the von Mises stress in Pa. TEMP is temperature in °C.*

A gravitational sag of 104.8 μm was measured at FNAL on a CMM with the actual completed layer 0 on supports at 1487 mm apart. Using these supports in the FEA model gave a predicted sag of 92.4 μm. There was no cooling fluid present in the test or the FEA model. Stresses in the structure were negligibly low, the von Mises stress being less than 2 MPa (Figure 10).

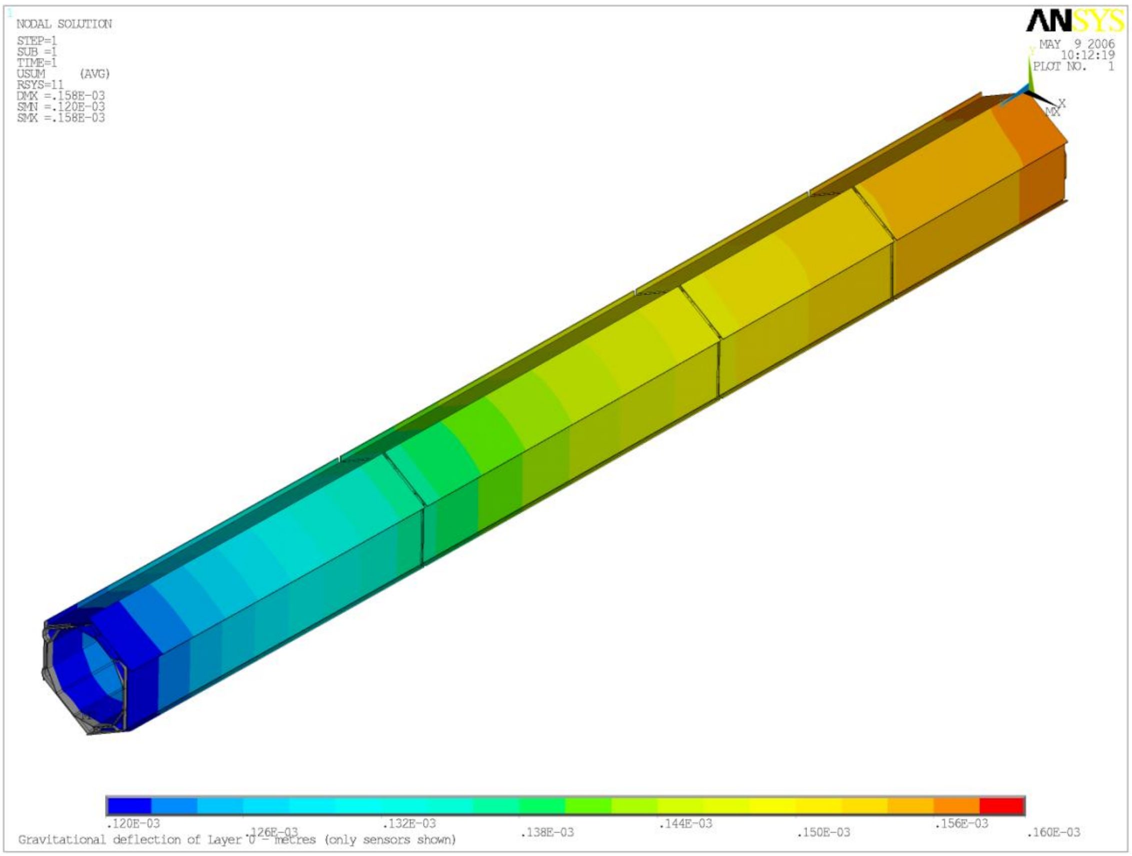

Figure 9: Gravitational Deflection in the Sensor Region. The Total Sagitta is 38 μm in This Region.

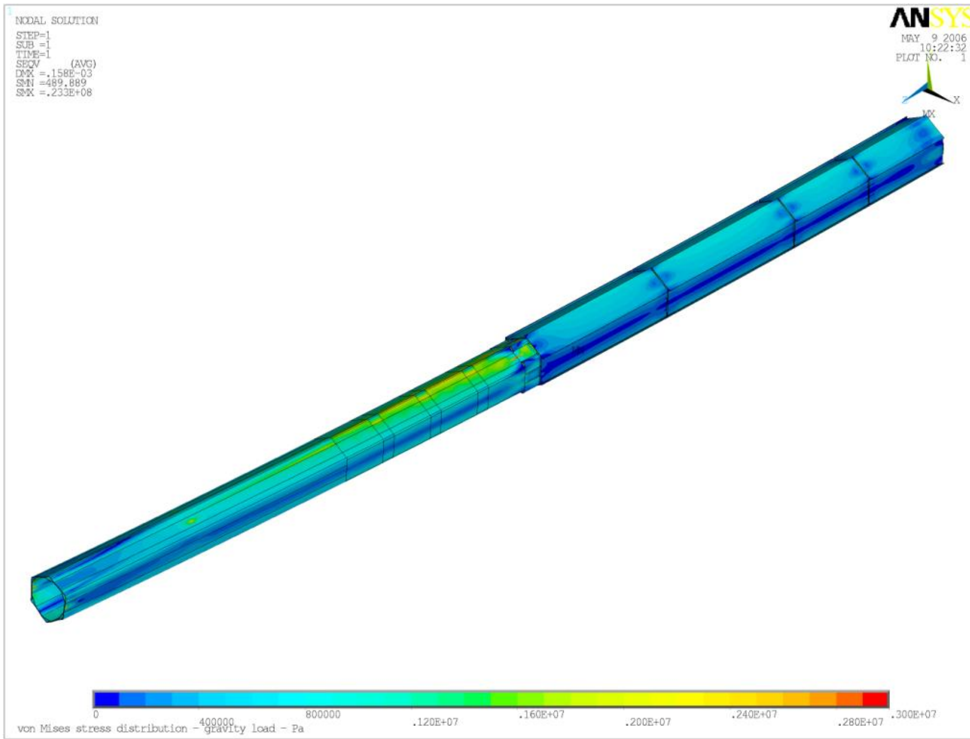

Figure 10: von Mises Stress in Layer0. The Maximum Stress is Negligible at 2 MPa.

L0 thermal

The temperature distribution in the L0 hybrids is shown in Figure 11 for a four hybrid section.

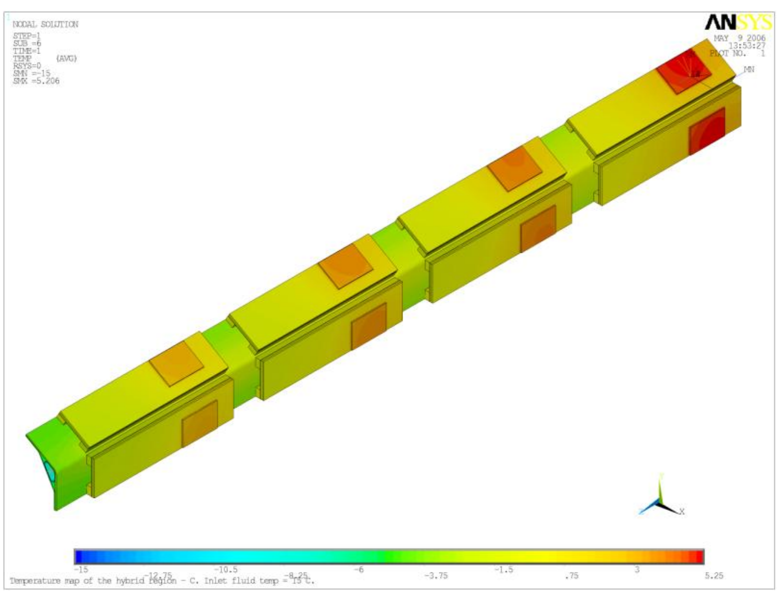

Figure 11: Temperature Distribution in Hybrid Region.

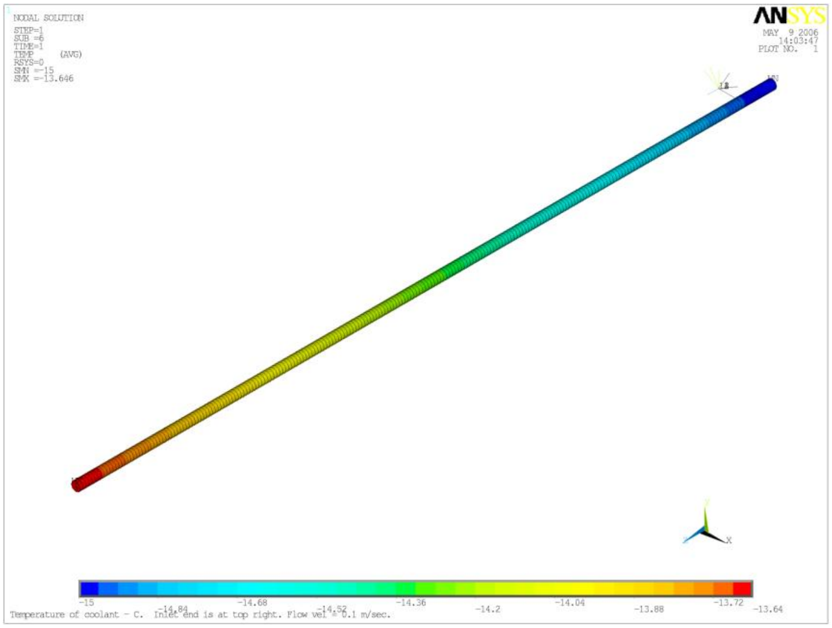

Figure 12: Temperature of Coolant in Hybrid Region.

Figure 12 shows the temperature of the coolant in the hybrid region as it flows along the tube. The temperature distribution through a cross section at the hybrid chips is shown in Figure 13. The temperature difference for this four hybrid model was 0.337 °C and the inlet temperature to the sensor region was -13.64 C.

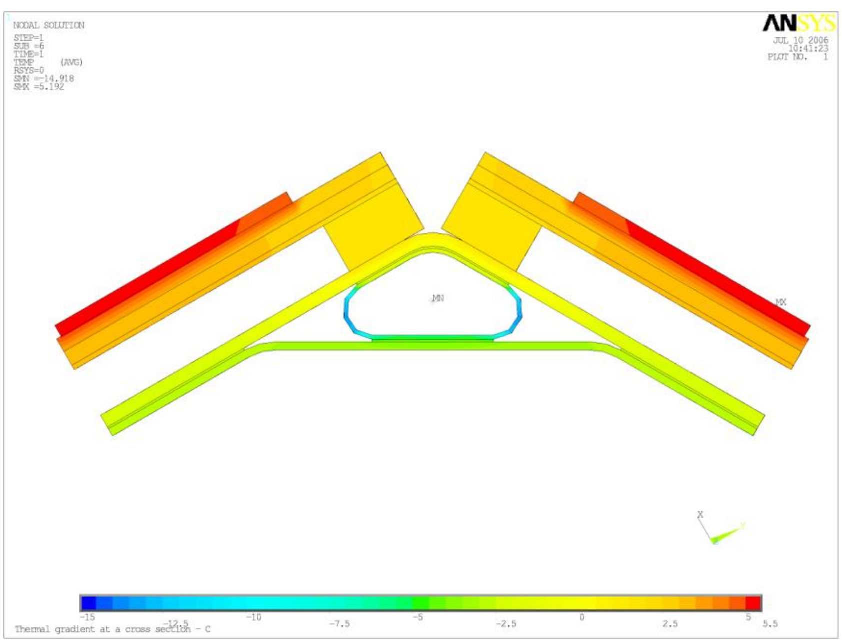

Figure 13: Temperature Through a Cross Section at a Hybrid.

Conclusions

The mechanical FEA results for L0 showed that the design goals of mechanical stiffness have been met and exceeded. This was due to the use of very high modulus carbon fibers and a fiber layup optimized to provide high bending stiffness of the structures. As expected, stresses in the structures were very low and were not a significant issue.

The thermal FEA results for L0 showed that the sensor temperatures were maintained at well below 0 °C and that only a very low flow rate of the coolant was required to maintain the desired temperature. The separately mounted hybrid chips have much less stringent temperature requirements and these were also easily met.

References:

1. ASTM Test Standard 3039, "Standard Test Method for Tensile Properties of Polymer Matrix Composite Materials", ASTM International, West Conshohocken, PA.

2. ASTM Test Standard 3518, "Standard Practice for IN-Plane Shear Response of Polymer Matrix Composite Materials by Tensile Test of a $\pm 45°$ Laminate", ASTM International, West Conshohocken, PA.

3. "The new Layer-0 Silicon Detector of the D-Zero Experiment", NIM (in preparation).

4. M.E. Tuttle, "Structural Analysis of Polymeric Composite Materials", Marcel-Dekker Inc, New York, NY, ISBN 0-8247-4717-8 (2004).